

MOTION GENERATION ON TRIM TRAJECTORIES FOR AN AUTONOMOUS UNDERACTUATED AIRSHIP

Salim HIMA, Yasmina BESTAOUI
Laboratoire des Systèmes Complexes, CNRS FRE 2492
Université d'Evry Val d'Essonne,
38 rue du pelvoux, 91020 Evry, France
tel : (33) 169-47-75-19; fax : (33) 169-47-75-99
E-mail : hima@cemif.univ-evry.fr and bestaoui@cemif.univ-evry.fr

Abstract : A blimp is a small airship that has no metal framework and collapses when deflated. In the first part of this paper, dynamic modeling of small autonomous non rigid airships is presented, using the Newton-Euler approach. This study discusses the motion in 6 degrees of freedom since 6 independent coordinates are necessary to determine the position and orientation of this vehicle. Euler angles are used in the formulation of this model. In the second part of the paper, path planning is introduced. Motion generation for trim trajectories is presented. This motion generation takes into account the dynamic model presented in the first part.

Key-words : Autonomous Airship, Trajectory planning, Underactuated systems, Nonholonomic systems

1. Introduction

Since their renaissance in early 1980's, airships have been increasingly considered for varied tasks such as transportation, surveillance, freight carrier, advertising, monitoring, research, and military roles. More recently, attention has been given to the use of unmanned airships as aerial inspection platforms, with a very important application area in environmental, biodiversity, and climatological research and monitoring [CAM99, KHO99, PAI99]. The first objective of this paper is to present a model of a small autonomous blimp : kinematics and dynamics. For kinematics, Euler angles are presented. For dynamics, a mathematical description of a dirigible flight must contain the necessary information about aerodynamic, structural and other internal dynamic effects (engine,

actuation) that influence the response of the blimp to the controls and external atmospheric disturbances. The blimp is a member of the family of under-actuated systems because it has fewer inputs than degrees of freedom. In some studies such as [FOS96, HYG00, KHO99, ZHA99], motion is referenced to a system of orthogonal body axes fixed in the airship, with the origin at the center of volume assumed to coincide with the gross center of buoyancy. The model used was written originally for a buoyant underwater vehicle [FOS96, ZIA98]. It was modified later to take into account the specificity of the airship [HYG00, KHO99, ZHA99]. In [BES01], the origin of the body fixed frame is the center of gravity.

The second objective of this paper is to generate a desired flight path and motion to be followed by the airship. A mission starts with take-off from the platform where the

mast that holds the mooring device of the blimp is mounted. Typically, flight operation modes can be defined as : take-off, cruise, turn, landing, hover...[BES01, CAM99, PAI99, ZHA99]. After the user has defined the goal tasks, the path generator then determines a path for the vehicle that is a trajectory in space. In this paper, the trajectories considered are trimming or equilibrium trajectories. The general condition for trim requires that the rate of change of the magnitude of the velocity vector is identically zero, in the body fixed frame. In this paper we propose some motion generation on trim helices to be followed by the airship.

2. AIRSHIP DYNAMIC MODELING

2.1. Kinematics.

A general spatial displacement of a rigid body consists of a finite rotation about a spatial axis and a finite translation along some vector. The rotational and translational axes in general need not be related to each other. It is often easiest to describe a spatial displacement as a combination of a rotation and a translation motions, where the two axes are not related. However, the combined effect of the two partial transformations (i.e rotation, translation about their respective axes) can be expressed as an equivalent unique screw displacement, where the rotational and translational axes in fact coincide. The concept of a screw thus represents an ideal mathematical tool to analyze spatial transformation [ZEF99]. The finite rotation of a rigid body does not obey to the laws of vector addition (in particular commutativity) and as a result the angular velocity of the body cannot be integrated to give the attitude of the body. There are many ways to describe finite rotations. Direction cosines, Rodrigues – Hamilton's (quaternions) variables [FOS96], Euler parameters [WEN91], Euler angles [BES01], can serve as examples. Some of these groups of

variables are very close to each other in their nature [ZEF99]. The usual minimal representation of orientation is given by a set of three Euler angles, assembled with the three position coordinates allow the description of the situation of a rigid body. A 3*3 direction cosine matrix (of Euler rotations) is used to describe the orientation of the body (achieved by 3 successive rotations) with respect to some fixed frame reference.

Two reference frames are considered in the derivation of the kinematics and dynamics equations of motion. These are the Earth fixed frame R_f and the body fixed frame R_m (figure 1). The position and orientation of the vehicle should be described relative to the inertial reference frame while the linear and angular velocities of the vehicle should be expressed in the body-fixed coordinate system. This formulation has been first used for underwater vehicles [FOS96, ZIA98].

In this paper, the origin C of R_m coincides with the center of volume of the vehicle. Its axes (x_v, y_v, z_v) are the principal axes of symmetry when available. They must form a right handed orthogonal normed frame.

The position and the orientation of the vehicle C in R_f can be respectively described by :

$$\eta_1 = \begin{pmatrix} x \\ y \\ z \end{pmatrix} \quad \eta_2 = \begin{pmatrix} \phi \\ \theta \\ \psi \end{pmatrix} \quad \text{eq 1}$$

with ϕ roll, θ pitch and ψ yaw angles.

The orientation matrix R is given by:

$$R = \begin{pmatrix} c_\psi c_\theta & -s_\psi c_\theta + c_\psi s_\theta s_\phi & s_\psi s_\theta + c_\psi s_\theta c_\phi \\ s_\psi c_\theta & c_\psi c_\theta + s_\psi s_\theta s_\phi & -c_\psi s_\theta + s_\psi s_\theta c_\phi \\ -s_\theta & c_\theta s_\phi & c_\theta c_\phi \end{pmatrix} \quad \text{eq 2}$$

Where $c_\theta = \cos(\theta)$ and $s_\theta = \sin(\theta)$

$R \in SO(3)$ denotes the orthogonal rotation matrix that specifies the orientation of the airship frame relative to the inertial

reference frame in inertial reference frame coordinates. $SO(3)$ is the special orthogonal group of order 3 which is represented by the set of all 3×3 orthogonal rotation matrices that characteristics are :

$$R^T R = I_{3 \times 3} \text{ and } \det(R) = 1 \quad \text{eq 3}$$

$I_{3 \times 3}$ represents the 3×3 identity matrix.

This description is valid in the region

$$-\frac{\pi}{2} < \theta < \frac{\pi}{2}. \text{ A singularity of this}$$

transformation exists for:

$$\theta = \frac{\pi}{2} \pm k\pi; k \in \mathbb{Z}.$$

If we use the manipulators formulation, at each instant, the configuration (position and orientation) of the airship can be described by an homogeneous transformation matrix corresponding to the displacement from frame R_f to frame

R_m . The set of all such matrices is called $SE(3)$, the special Euclidean group of rigid-body transformations in three dimensions [SEL96].

$$SE(3) = \left\{ A \mid A = \begin{bmatrix} R & \eta_1 \\ 0 & 1 \end{bmatrix}, R \in SO(3) \subset \mathfrak{R}^{3 \times 3} \right. \\ \left. \eta_1 \in \mathfrak{R}^3; R^T R = I_{3 \times 3}; \det(R) = 1 \right\} \quad \text{eq 4}$$

$SE(3)$ is a Lie group. \mathfrak{R}^3 represents the set of 3×1 real vectors and $\mathfrak{R}^{3 \times 3}$ the set of 3×3 real matrices.

Let's introduce $V = \begin{pmatrix} u \\ v \\ w \end{pmatrix}$ as the linear

velocity of the origin C expressed in R_m

and $\Omega = \begin{pmatrix} p \\ q \\ r \end{pmatrix}$ as the angular velocity

expressed in R_m . The kinematics of the airship can be expressed in the following way :

$$\begin{pmatrix} \dot{\eta}_1 \\ \dot{\eta}_2 \end{pmatrix} = \begin{pmatrix} R & 0_{3 \times 3} \\ 0_{3 \times 3} & J(\eta_2) \end{pmatrix} \begin{pmatrix} V \\ \Omega \end{pmatrix} \quad \text{eq 5}$$

where

$$J(\eta_2) = \begin{pmatrix} 1 & s\phi \cdot \tan \theta & c\phi \cdot \tan \theta \\ 0 & c\phi & -s\phi \\ 0 & s\phi / c\theta & c\phi / c\theta \end{pmatrix} \quad \text{eq 6}$$

If we use the metric formulation, the tangent space of $SE(3)$, denoted by $se(3)$ is given by:

$$se(3) = \left\{ \begin{bmatrix} sk(\Omega) & V \\ 0 & 0 \end{bmatrix}; sk(\Omega) \in \mathfrak{R}^{3 \times 3}; V \in \mathfrak{R}^3 \right\} \quad \text{eq 7}$$

where $sk(\Omega)$ represents the skew-matrix :

$$sk(\Omega) = \begin{bmatrix} 0 & -r & q \\ r & 0 & -p \\ -q & p & 0 \end{bmatrix}$$

This matrix has the property that for an arbitrary vector $U \in \mathfrak{R}^3$

$$sk(\Omega)U = \Omega \times U \quad \text{eq 8}$$

\times : represents the cross vector product in \mathfrak{R}^3 .

This tangent space $se(3)$ has the structure of a Lie algebra.

2.2. Dynamics.

In this section, analytic expressions for the forces and moments on the dirigible are derived. It is advantageous to formulate the equations of motion in a body fixed frame to take advantage of the vehicle's geometrical properties. Applying Newton's laws of motion relating the applied forces and moments to the resulting translational and rotational accelerations assembles the equations of motion for the 6 degrees of freedom. The forces and moments are referred to a system of body-fixed axes, centered at the airship center of volume. We will make in the sequel some simplifying assumptions : the earth fixed

reference frame is inertial, the gravitational field is constant, the airship is supposed to be a rigid body, meaning that it is well inflated, the aeroelastic effects are ignored, the density of air is supposed to be uniform, and the influence of gust is considered as a continuous disturbance, ignoring its stochastic character [MIL73, TUR73]. The deformations are considered to be negligible. The buoyancy system lifetime will be limited by a number of components and factors. Included is the corrosion of unprotected airship skin, degradation of the airship skin due to thermal cycling and temperature exposure and buoyant gas leakage. High temperature will increase permeability of the airship skin and increase leakage. Introducing all these factors into the dynamic model would result in very complicated partial differential equations. Assume that the airship move in a trim manner and the flight mode is aerostatics, then the buoyancy is compensated by the weight force, the aerodynamic forces can be neglected as well as the different linear and angular accelerations in the body fixed frame. Let's assume that the forces developed by the two vectored lateral helices are equal $F_1 = F_2 = F$. The dynamics model is expressed in the body fixed frames as [HYG00]:

Forces equations :

Axial force :

$$\begin{aligned} 2F \cos(\mu) &= m_z wq - m_y rv \\ -m(a_x(q^2 + r^2) - a_z rp) \end{aligned} \quad \text{eq 9}$$

Lateral force :

$$F_3 = -m_x ur + m_z wp + m(-a_x pq + a_z rq) \quad \text{eq 10}$$

Normal force :

$$\begin{aligned} 2F \sin(\mu) &= -m_y vp + m_x qu \\ +m(-a_x rp + a_z(q^2 + p^2)) \end{aligned} \quad \text{eq 11}$$

Moment equations :

Roll moment :

$$\begin{aligned} F_3 O_{3z} &= (J_z - J_y)rq - I_{xz}pq - ma_z(ur - pw) \\ +a_z F_G \cos(\theta) \sin(\phi) \end{aligned} \quad \text{eq 12}$$

Pitch moment :

$$\begin{aligned} FO_x \sin(\mu) - FO_z \cos(\mu) &= -(J_x - J_z)pr \\ +I_{xz}(r^2 - p^2) + m(a_x(vp - qu) - a_z(wq - rv)) \\ -a_z F_G \sin(\theta) - a_x F_G \cos(\theta) \cos(\phi) \end{aligned} \quad \text{eq 13}$$

Yaw moment :

$$\begin{aligned} F_3 O_{3x} &= (J_z - J_y)qp + I_{xz}qr \\ -m(-a_x(ur - pw)) - a_x F_G \cos(\theta) \sin(\phi) \end{aligned} \quad \text{eq 14}$$

where :

O_{ij} is the j th coordinate of the origin of the actuator i .

$$O_x = O_{1x} + O_{3x} \quad \text{and} \quad O_z = O_{1z} + O_{3z}.$$

From these equations we can derive 3 nonholonomic constraints :

First nonholonomic constraint:

$$\begin{aligned} (O_{3z}M_x + Ma_z)ru - (O_{3z}M_z + Ma_z)pw \\ -M(a_x pq + a_z rq) - (J_z - J_y)rq + I_{xz}pq \\ -a_z Fg \cos(\theta) = 0 \end{aligned} \quad \text{eq 15}$$

Second nonholonomic constraint:

$$\begin{aligned} (O_{3x}M_x + Ma_x)ru - (O_{3x}M_z + Ma_x)pw \\ -MO_{3x}(a_z rq - a_x pq) - (J_y - J_x)qp \\ -I_{xz}pr + a_x Fg \cos(\theta) \sin(\phi) = 0 \end{aligned} \quad \text{eq 16}$$

Third nonholonomic constraint:

$$\begin{aligned} & \frac{1}{2}O_z(M_z wq - M_y rv - M(a_x(q^2 + r^2) - a_z rp)) \\ & - \frac{1}{2}O_x(M_x qu - M_y vp + M(a_z(q^2 + p^2) - a_x rp)) \text{ eq 17} \\ & - (J_x - J_z)pr - I_{xz}(r^2 - p^2) \\ & - M(a_x(vp - uq) - a_z(wq - vr)) \\ & - a_z Fg \sin(\theta) + a_x Fg \cos(\theta) \cos(\phi) = 0 \end{aligned}$$

3. Trim trajectories

3.1. Path generation

The fundamentals of flight are in general : straight and level flight (maintenance of selected altitude), ascents and descents, level turns, wind drift correction and ground reference maneuvers. Trim is concerned with the ability to maintain flight equilibrium with controls fixed. A trimmed flight condition is defined as one in which the rate of change (of magnitude) of the aircraft's state vector is zero (in the body-fixed frame) and the resultant of the applied forces and moments is zero. In a trimmed maneuver, the aircraft will be accelerated under the action of non-zero resultant aerodynamic and gravitational forces and moments, these effects will be balanced by effects such as centrifugal and gyroscopic inertial forces and moments. The trim problem is generally formulated as a set of nonlinear algebraic equations.

$$\dot{u} = \dot{v} = \dot{w} = \dot{p} = \dot{q} = \dot{r} = 0$$

Using eq 5, the angular velocity can be written as:

$$\begin{aligned} p &= \dot{\phi} - \psi S\theta \\ q &= \dot{\theta} C\phi + \psi S\phi C\theta \\ r &= -\dot{\theta} S\phi + \psi C\phi C\theta \end{aligned} \text{ eq 18}$$

differentiating versus time and nullifying these derivatives, we obtain

$$\begin{aligned} p_0 &= -\psi_0 S\theta_0, \\ q_0 &= \psi_0 C\theta_0 S\phi_0 \\ r_0 &= \psi_0 C\theta_0 C\phi_0 \end{aligned} \text{ eq 19}$$

with one of the solutions given by :

$$\begin{pmatrix} \dot{\phi} = 0 \\ \dot{\theta} = 0 \\ \dot{\psi} = cst = \psi_0 \end{pmatrix} \text{ eq 20}$$

thus

$$\begin{pmatrix} \phi = cst = \phi_0 \\ \theta = cst = \theta_0 \\ \psi = \psi_0 t \end{pmatrix} \text{ eq 21}$$

from the same equation Eq 5, trimming trajectories are characterized by :

$$\begin{aligned} x &= a_x \cos(\psi_0 t) + b_x \sin(\psi_0 t) \\ y &= a_y \cos(\psi_0 t) + b_y \sin(\psi_0 t) \\ z &= z_0 = -\sin(\theta_0)u_0 + \cos(\theta_0)\sin(\phi_0)v_0 + \cos(\theta_0)\cos(\phi_0)w_0 \end{aligned} \text{ eq 22}$$

where

$$\begin{aligned} a_x &= \cos(\theta_0)u_0 + \sin(\theta_0)\sin(\phi_0)v_0 + \sin(\theta_0)\cos(\phi_0)w_0 \\ b_y &= a_x \\ b_x &= -\cos(\phi_0)v_0 + \sin(\phi_0)w_0 \\ a_y &= -b_x \end{aligned} \text{ eq 23}$$

Integrating, we obtain

$$r(s) = \begin{pmatrix} x(s) \\ y(s) \\ z(s) \end{pmatrix} \text{ eq 24}$$

with

$$\begin{aligned}
x &= \frac{a_x}{V_e} \sin\left(\frac{\psi_0}{V_e} s\right) - \frac{b_x}{V_e} \cos\left(\frac{\psi_0}{V_e} s\right) \\
y &= -\frac{b_x}{V_e} \sin\left(\frac{\psi_0}{V_e} s\right) - \frac{a_x}{V_e} \cos\left(\frac{\psi_0}{V_e} s\right) \\
z &= \frac{z}{V_e} s
\end{aligned} \tag{eq 25}$$

where s represents the curvilinear abscissa and we suppose a uniform motion such that

$$s = V_e t = t \sqrt{u_0^2 + v_0^2 + w_0^2} \tag{eq 26}$$

the trajectories represented by these equations are helices with constant curvature and torsion. The most general trim condition resembles a spin mode. The spin axis is always directed vertically in the trim and pass through the origin of \mathcal{R}_f .

The trim condition can be a turning (about the vertical axis), descending or climbing (assuming constant air density and temperature), side-slipping maneuver at constant speed. More conventional flight conditions such as hover, cruise, auto-rotation or sustained turns are also trims.

3.2. Motion generation : Problem formulation

Once the path is planned, we are looking for the form of the motion that allows the airship to move along this path in a minimum time and a safe manner (without slipping or excitation of the harmful modes such as a roll oscillation). Since the linear velocity is constant, the optimal time solution for this problem have minimum paths length. We may propose an optimization problem where the objective function may be a mixed time energy function

The total time can be expressed as:

$$T_f = \frac{z_f - z_i}{-\sin\theta.u + \cos\theta.\sin\phi.v + \cos\theta.\cos\phi.w} \tag{eq 27}$$

while the energy is given by :

$$E = (F^2 + F_3^2).T_f \tag{eq 28}$$

The overall problem consists now in determining some variables $\begin{pmatrix} u & v & w & \dot{\psi} \end{pmatrix}$

to minimize the specified objective function: mixed time-energy subject to three equality constraints (dynamics) and inequality constraints (actuators).

$$\begin{aligned}
\min & \quad \lambda T_f + (1-\lambda)E \\
\text{subject to} & \quad |F| \leq F_{\max} \quad |F_3| \leq F_{3\max} \\
& \quad \mu_{\min} \leq \mu \leq \mu_{\max}
\end{aligned} \tag{eq 29}$$

A proposed resolution method is introduced in the following section.

3.3. Resolution of the minimum time problem

Optimization theory gives a solution to the minimum time problem. It is located on the boundary of the admissible set, i.e. the airship moves using maximum actuator capabilities. The resolution will be organized as follows. First, this problem will be solved assuming that each constraint is saturated. Then the largest value of all the computed times will be taken as the predicted arrival time. In the first instance, we solve the three equality constraints (eq 39, eq 41, eq 42), this allows us to obtain $\begin{pmatrix} u & v & w \end{pmatrix}$ versus

$\dot{\psi}$. The multi-variable optimization problem becomes now a mono-variable optimization problem. Applying the second order necessary and sufficient conditions, we have to solve a set of five nonlinear equations.

$$\begin{aligned}
F^2 &= F_{\max}^2 & F_3 &= \pm F_{3\max} \\
\mu &= \mu_{\min} & \mu &= \mu_{\max}
\end{aligned} \tag{eq 30}$$

$$\begin{aligned}
\text{Solving } & F_3 = \pm F_{3\max} \\
& \mu = \mu_{\min} \quad \mu = \mu_{\max}
\end{aligned}$$

lead to four simple second order polynomial equation of the form ;

$$A_0 \dot{\psi}^2 + A_1 = 0$$

Solving $F^2 = F_{\max}^2$ leads to a fourth order polynomial equation of the form;

$$B_4 \dot{\psi}^4 + B_2 \dot{\psi}^2 + B_0 = 0$$

where the coefficients A and B are constants dependent on the parameters of the dynamic model and the initial and final configurations. We obtain two imaginary solutions, one real positive and one real negative. Depending on our goals and constraints, we choose the positive or negative solution.

Thus the solution of the optimization problem can be found analytically.

3.4. Resolution of the mixed problem

In this section we treat the problem of finding helices, as well as the motion, that minimize both time and energy. The cost function is given by :

$$J = J_E + J_t = (F^2 + F_3^2)T_f + T_f$$

the form of the cost function is valid in the sense that multiplying the square of the forces by the time rather than integrating them with respect of the time because trim trajectories imply a constant forces. simplification can be made on these equation to formulate this equation in the form of rational polynomial equation done by :

$$J = \frac{\sum_{i=0}^6 a_{num,k} \left(\dot{\psi} \right)^i}{\sum_{k=0}^2 a_{den,k} \left(\dot{\psi} \right)^k}$$

differentiate J and nullifying its denominator lead to seven order polynomial equation :

$$\frac{\partial J}{\partial \dot{\psi}} = \sum_{i=0}^7 b_i \left(\dot{\psi} \right)^i$$

from the seven solution derived from the last equation, we take that present a minimal cost.

4. SIMULATION RESULTS

The lighter than air platform is the AS200 by Airspeed Airships. It is a remotely piloted airship designed for remote sensing. It is a non rigid 6m long, 1.4m diameter and 8.6 m^3 volume airship equipped with two vectorable engines on the sides of the gondola and 4 control surfaces at the stern. The four stabilisers are externally braced on the full and rudder movement is provided by direct linkage to the servos. Envelope pressure is maintained by air fed from the propellers into the two ballonets located inside the central portion of the hull. These ballonets are self regulating and can be fed from either engine. The engines are standard model aircraft type units, The propellers can be rotated through 120 degrees. During flight the ruddervators (Rudder and elevator) are used for all movements in pitch and yaw. In addition, the trim function can be used to alter the attitude of the airship in order to obtain level flight or to fly with a positive or negative pitch angle.

Rudder and elevator can be moved from -25 to $+25$ degrees. The maximum velocity is 13m/s and the maximal height is 200m. Climb or dive angles should not exceed 30 degrees, particularly at full throttle.

For the following initial conditions:

$$\theta = 0.44 \text{ rad}; \varphi = 0.3 \text{ rad}$$

we obtain the following linear and angular velocities ;

$$\begin{pmatrix} u = 2.57 \\ v = -4.35 \\ w = -2.62 \end{pmatrix} m/s \quad \begin{pmatrix} p = -1.59 \\ q = 1 \\ r = 3.23 \end{pmatrix} rad/s$$

The trim values for the inputs are :

$$F_{trim} = 100N; F_{3trim} = -13.53N; \mu_{trim} = -0.43rad$$

Figure 2 presents the trim trajectory: a helix with constant curvature and torsion, while figure 3 presents its projection on the x-y plane. Figure 4 presents respectively

the angles (θ, ϕ, ψ) and figure 5 the derivatives : $\begin{pmatrix} \dot{x} & \dot{y} & \dot{z} \end{pmatrix}$.

Depending on the initial conditions, we have to consider the propulsion constraints on a given order. The most basic constraint is the limitation of the main thruster, then we have to consider either the constraint on the tail thruster or the tilt angle. Figure 6 shows the set of initial conditions (θ, ϕ) usable for a forward flight when considering only the limitation on F, while figures 7 and 8 show respectively, the set of initial conditions when we add the constraint on the tail thruster and the tilt angle.

5. CONCLUSIONS

Airships are a highly interesting study object due to their stability properties. The classical theory of airship stability and control is based on a linearised system of differential equations usually obtained by considering small perturbations about a steady flight condition. However, the constraints of staying within the linear flight regime are excessive. The design of advanced control system must take into account the strong non linearities of the dynamic model. In this prospect, in the first part of this paper, we have discussed kinematics and dynamics of an airship, using Newton Euler approach. A direct generalization of this model is to introduce the effects of the vertical and horizontal control surfaces.

In the second part of this paper, we have discussed characterisation of some helices for airships. Trimming trajectories have been presented. They consist in helices with constant curvature and torsion. When specifying a trajectory, the physical limits of the system must be taken into account. For trim flights, we propose a motion generation problem by minimizing the traveling time, given

realistic constraints, the generated forces and the tilt angle.

Our future prospect is how to steer the configuration of a mechanical system from one point to another in 3D.

BIBLIOGRAPHY

[BES01] **Y. Bestaoui, S. Hima** ‘Some insights in path planning of small autonomous blimps’ Archives of control sciences, Polish Academy of Sciences, volume 11 (XLVII), 2001, #3-4, pp.21-49.

[CAM99] **M. F. M. Campos, L. de Souza Coelho** ‘Autonomous dirigible navigation using visual tracking and pose estimation’ IEEE international Conference on Robotics and Automation, Detroit, MI, May 1999, pp. 2584 – 2589.

[FOS96] **T. Fossen** ‘Guidance and control of ocean vehicles’ J. Wiley press, 1996.

[HYG00] **E. Hygounec, P. Soueres, S. Lacroix** ‘Modelisation d’un dirigeable, Etude de la cinématique et de la dynamique’ CNRS report #426, LAAS, Toulouse, France, Oct. 2000.

[KHO99] **G. A. Khoury, J. D. Gillet, eds.** ‘Airship technology’ Cambridge university press, 1999.

[MIL73] **L. M. Milne** ‘Theoretical aerodynamics’ Dover Publications, 1973.

[PAI99] **E. C. de Paiva, S. S. Bueno, S. B. Gomes, J. J. Ramos, M. Bergerman** ‘A control system development environment for AURORA’s semi-autonomous robotic airship’ IEEE international Conference on Robotics and Automation, Detroit, MI, May 1999, pp. 2328 – 2335.

[RAB00] **P. J. Rabier, W. C. Rheinboldt** ‘Nonholonomic motion of rigid mechanical systems from a DAE viewpoint’ SIAM press; 2000.

[SEL96] **J. M. Selig** ‘Geometrical methods in robotics’ Springer-verlag, 1996.

[TUR73] J. S. Turner ‘Buoyancy effects in fluids’ Cambridge University Press, 1973.

[WEN91] J. T. Y. Wen, K. Kreutz – Delgado ‘The attitude control problem’ IEEE Transactions on Automatic Control, vol 36, #10, 1991, pp. 1148-1161.

[ZHA99] H. Zhang, J. P. Ostrowski ‘Visual servoing with dynamics : Control of an unmanned blimp’ IEEE international Conference on Robotics and Automation, Detroit, MI, May 1999, pp. 618 – 623.

[ZEF99] M. Zefran, V. Kumar, C. Croke ‘Metrics and connections for rigid-body kinematics’ International Journal of Robotics Research, vol. 18, #2, feb. 1999, pp. 243-258.

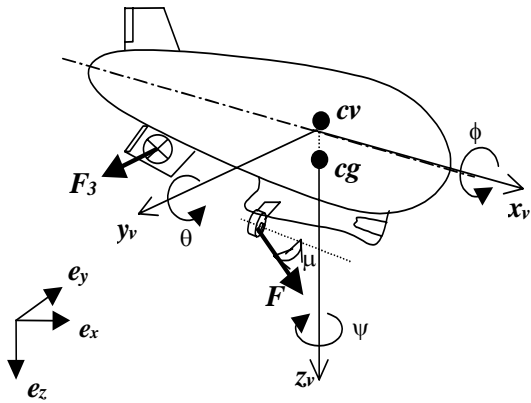


Figure 1

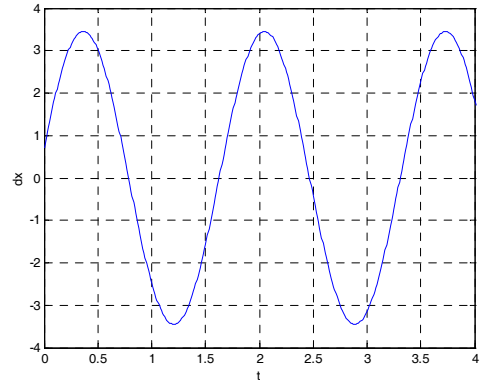


Figure 4 : \dot{x}

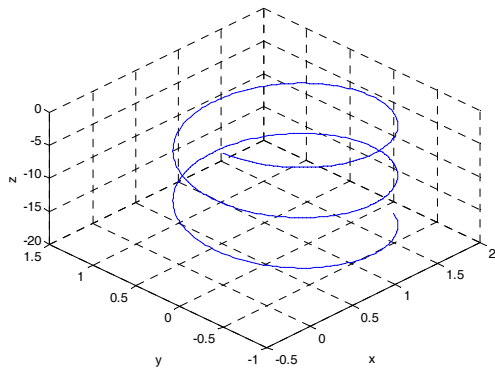


Figure 2 : 3D helix

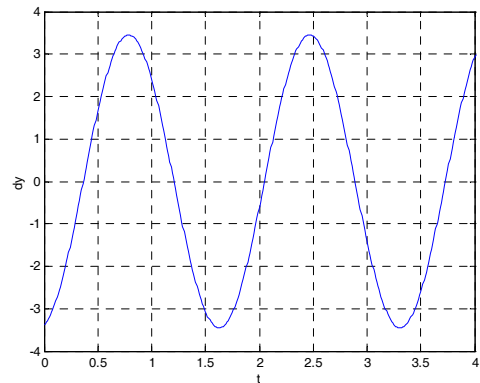


Figure 5 : \dot{y}

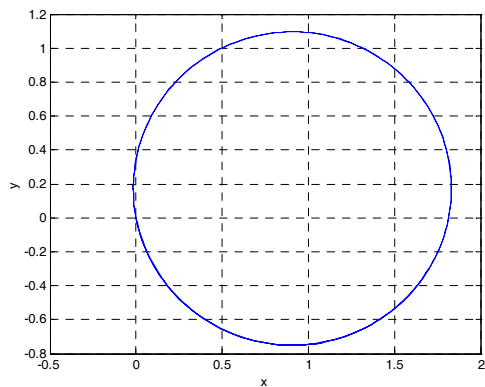


Figure 3 : projection in the x-y plane

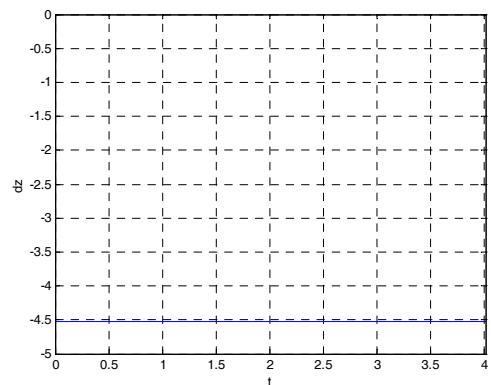


Figure 6 : \dot{z}

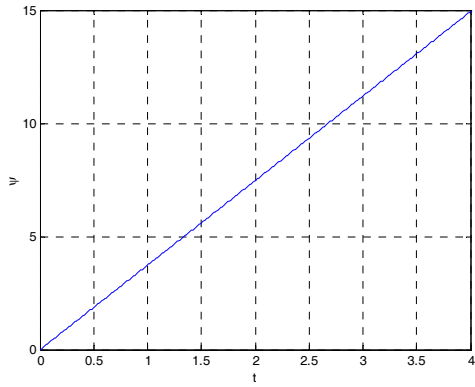


Figure 7 : the angle ψ

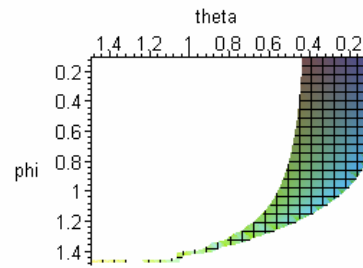


Figure 9 : possible initial conditions for $F=F_{\max}$ and $\mu \leq \mu_{\max}$

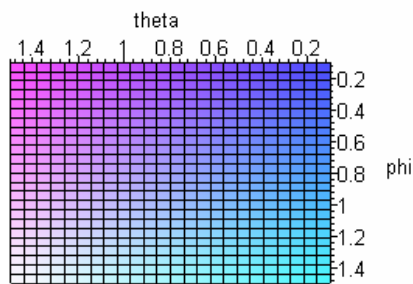


Figure 8 : possible initial conditions for $F=F_{\max}$

Mixed cost simulation results

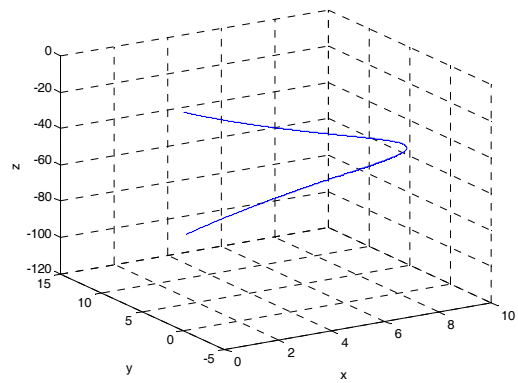


Figure 10 : 3D helix

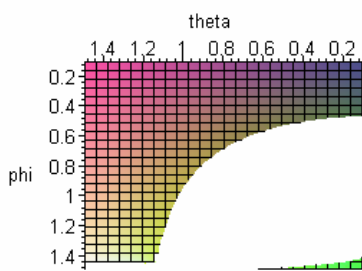


Figure 9 : possible initial conditions for $F=F_{\max}$ and $F_3 \leq F_{3\max}$

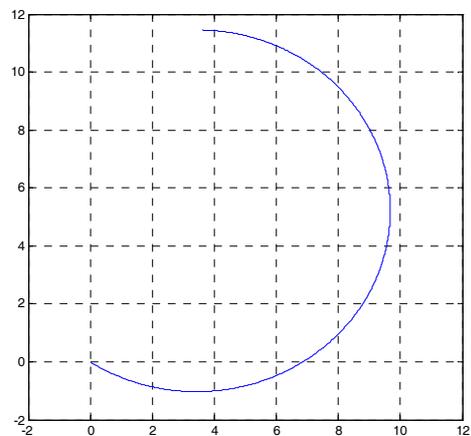


Figure 10 : projection in the x-y plane

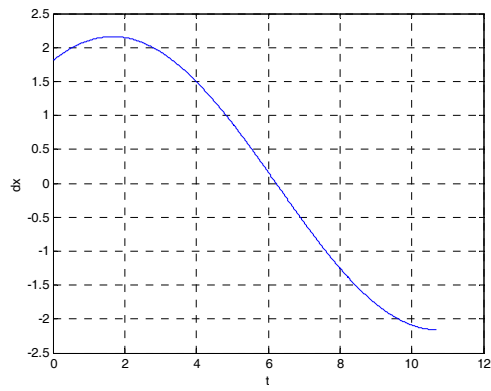


Figure 10 : \dot{x}

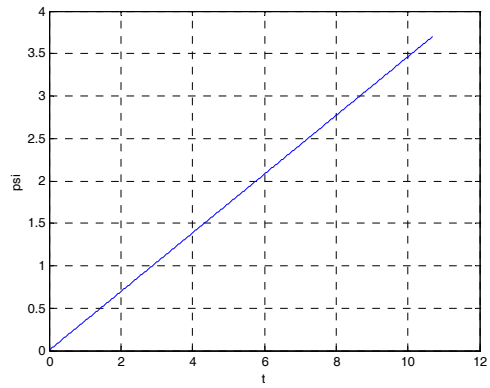


Figure 13 : ψ

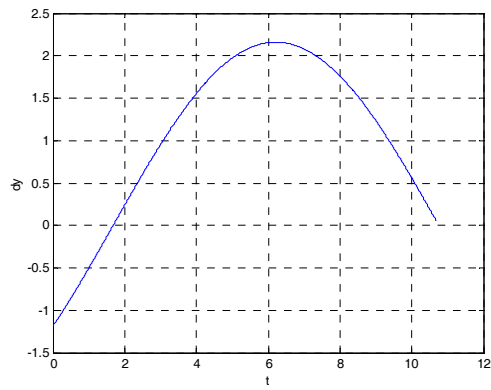


Figure 11 : \dot{y}

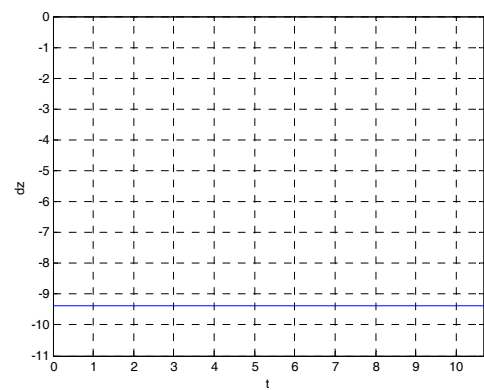


Figure 12 : \dot{z}